Academic Article

Making Climatic Zoning Maps in Yokohama -Comparison among different resolution calculations-

Makoto Yokoyama*[1] Takahiro Tanaka*[1] Toru Sugiyama*[2] Satoru Sadohara*[3]

*[1] Graduate School of Engineering, Hiroshima University
*[2] Center for Earth Information Science and Technology, Japan Agency for Marine-Earth Science Technology
*[3] Graduate School of Urban Innovation, Yokohama National University

Corresponding author: Makoto Yokoyama, yokomako.3918@gmail.com

ABSTRACT

Although countermeasures against urban warming and its effects have been studied in recent years, these countermeasures must be introduced into a suitable place for effective urban environmental planning. Therefore, classification of urban areas in zoning maps must be done in terms of climatic environments to find necessary and effective countermeasures for respective zones.

Numerical calculations using a meso-scale meteorological model are often used to produce such maps. This study calculated the climatic environment in Yokohama at 500 m resolution and at 100 m resolution, respectively, using a WRF (Weather Research and Forecasting) model and an MSSG (Multi-Scale Simulator for the Geoenvironment) model. These calculation results were then compared with observations. Calculation accuracy of relative magnitude correlation of these calculations were compared to analyze whether high-resolution calculation is effective or not for making climatic zoning maps. Furthermore, climatic zoning maps were produced from these calculation results and cluster analyses. Results show that urban areas in Yokohama are classifiable into five zones in terms of patterns of air temperature change. Additionally, more detailed effects can be incorporated into climatic zoning maps using high-resolution calculations with an MSSG model.

Key Words *: Climatic zoning map, Air temperature, Numerical calculation, Cluster analysis, Sea breeze*

1. Introduction

In recent years, the thermal environment in urbanized areas is becoming increasingly inhospitable for residents because of urban heat island effect and global warming. These phenomena are collectively regarded as urban warming. Many countermeasures against urban warming such as improving wind ventilation and increasing the green ratio in urban areas and its effects have been studied. However, these countermeasures should be introduced into suitable places for effective urban environmental planning.

From this background, urban environmental climate maps [(1)] are proposed as effective tools to inform urban planning stakeholders such as urban planners, architects, and residents about the urban environment. As one layer of urban environmental climate maps, zoning maps classifying urban areas in terms of urban climate are necessary for presenting and considering effective countermeasures for each zone. Making such maps necessitates classification of target areas into some zones in terms of urban climate. Using results of numerical calculation is apparently effective for such classification. Meso-scale meteorological models are often used to elucidate spatial characteristics of urban climatic environments [(2)(3)]. Such models are regarded as useful to produce climatic zoning maps.

As previous research related to making climatic zoning map based on result of meso-scale meteorological model, Kitao et al.[(4)] calculated climatic environment of Osaka region with 1km resolution by using Weather Research and Forecalting (WRF) model and made regional climate atlas in Osaka region for suggesting the pro-environmental urban plannning. Oba et al.[(5)] analysed the spatial distribution of heat budget inside Sendai and made “heat balance map” with 500m resolution. In addition, climatic zoning to select appropriate countermeasures against heat island effects based on this map was proposed. Matsuo and Tanaka[(6)] analysed the effect of sea breeze on summer diurnal

temperature in Hiroshima plain for mapping the sea breeze effect for mitigating urban warming. In this study, definite zoning is not defined but spatial distribution of sea breeze effect is calculated with 1km resolution. As shown in these studies, the spatial resolution of climatic zoning based on numerical calculation is rough because of constraints of computation time, and other restrictions.

Generally, climate zoning with reflecting detailed effects such as topography and land use. But, these effect is also important for making zoning maps in some citis having complicated topography.

However, high-resolution calculations for wider areas can be executed using supercomputers in recent years. A Multi-Scale Simulator for the Geoenvironment (MSSG) model can be developed for multi-scale calculation in the Earth Simulator. This model can execute such high-resolution calculations for a wider area. Therefore, more detailed climatic zoning maps can be anticipated using this model.

For this study, calculations of two kinds were executed respectively using WRF model and MSSG model. These calculation results are compared with observation results. Then calculation accuracy of relative magnitude correlation of these calculations were compared to analyze whether high-resolution calculation is effective or not for making climatic zoning maps. Additionally, climatic zoning maps are produced from these calculation results. Urban areas in Yokohama are classified into five zones in terms of air temperature change patterns using cluster analysis.

2. Research outline

2.1 Target area

For this study, Yokohama was selected as the target area. Figure 1 portrays locations and topographical characteristics of the target area. Yokohama, a hilly city, has many small valleys called “yato” throughout the whole city area. Urban areas extend throughout the whole city area; urban heat island effect has been reported there [7]. However, Yokohama faces Tokyo Bay and is located near Sagami Bay. Figure 2 shows wind roses of AMeDAS Tsujido and the Yokohama Local Meteorological Observatory (YLMO). Locations of these observation points are presented in Figure 1. As shown in Figure 2, a south wind blows at both points. An east wind blows at YLMO during the daytime. Therefore, it is considered that the sea breeze effect mitigates urban warming in this area.

In addition, fine weather days are classified into three groups (i.e. day without southwest wind, day with southwest wind and

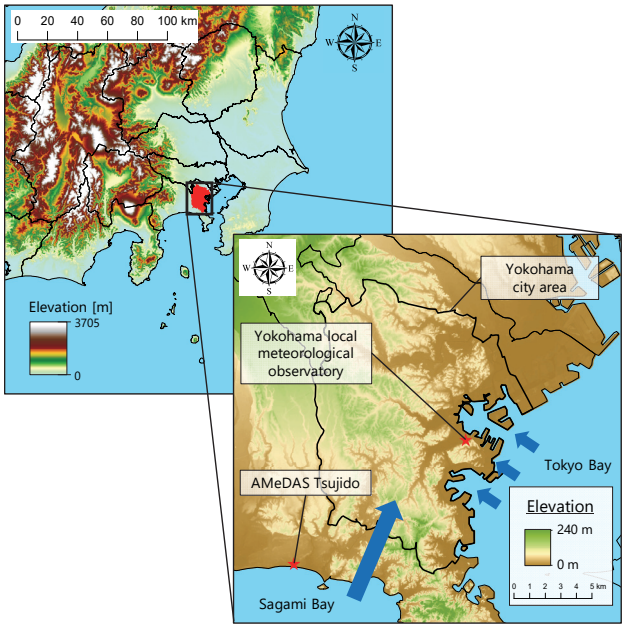

Fig. 1 Yokohama location and topography. This area is located near Sagami Bay, facing Tokyo Bay.

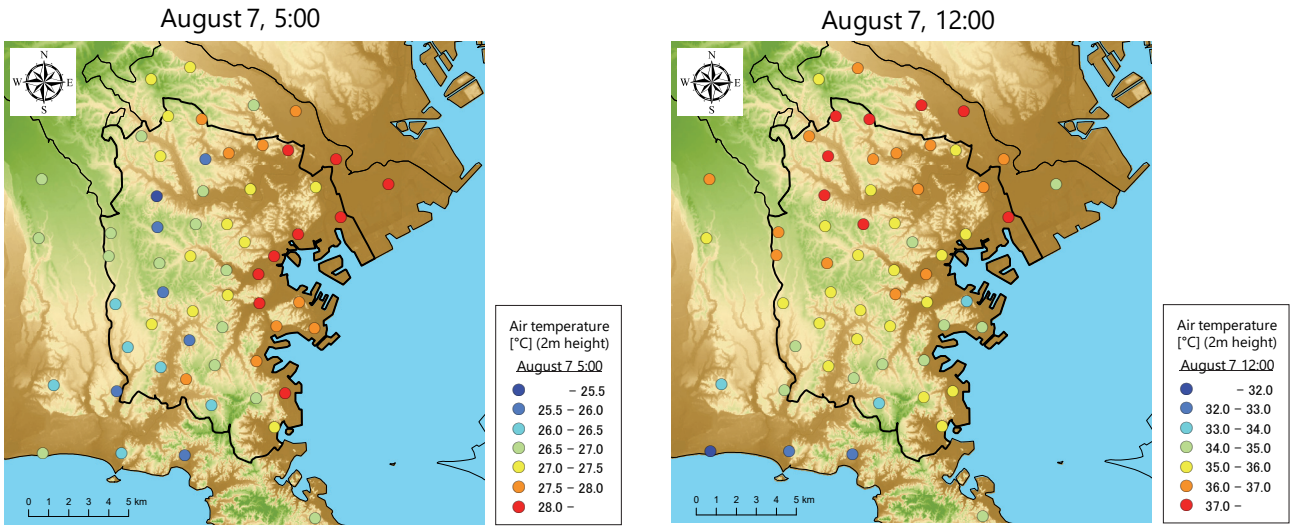

Fig. 3 Hourly averaged air temperature distribution of August 7 (left) 5:00 JST, (right) 12:00 JST. Air temperatures in Yokohama are higher around the eastern coastal area at 5:00 JST and higher around the northwestern part at 12:00.

day with both east and southwest wind) by sea breeze blowing patterns among this area[8]. Especially, number of days with both east and southwest wind is largest in these three patterns in summer of 2015. Therefore, August 7 in 2015 is selected as a target day in this study. This day is a typical sunny day and the end of continuous fine weather days period. East wind blows in the morning and southwest wind blows in the afternoon according to observatonal data at YLMO. Analysis on other days and other sea breeze blowing patterns are next steps.

Basic information related to Yokohama is given as shown below.

- Area: 437.4 [km^2]
- Population: 3,728,124 [persons] (2015)

2.2 Meteorological observations

For this study, 59 air temperature sensors were set in and around Yokohama for the observation period of July 24 through August 31 in 2015. Observations were recorded at 10 min intervals. All sensors were set in Stevenson screens located at elementary schools throughout Yokohama. Figure 3 shows the air temperature distribution at 5:00 JST and 12:00 JST on August 7. In the daytime, the southern part of the city is cooler; the northern part is hotter. Furthermore, the maximum air temperature in that time reaches to over 37 °C. Therefore, it seems that the air temperature distribution during the daytime is affected by the air temperature reduction effect of the sea breeze, especially from Sagami Bay in this area. In the nighttime, the eastern part is hotter; the inland area is cooler. This distribution pattern is apparently affected by the seawater temperature, land cover, and anthropogenic heat from factory areas in the coastal area of Tokyo Bay.

2.3 Calculation conditions

In this study, two resolution cases were calculated. Case A was calculated using a Weather Research & Forecasting (WRF) model with 500 m resolution. The WRF model is a popular meso-scale meteorological model used worldwide [9]; WRF ver. 3.7.1 was used for this study. Case B was calculated using an MSSG model with 100 m resolution. An MSSG model is multiscale atmospheric-ocean coupled model developed by the Center for Earth Information Science and Technology, Japan Agency for Marine–Earth Science and Technology (JAMSTEC). An MSSG model can execute global, meso, and urban scale numerical calculations [10]. For this study, we used meso-scale components of this model.

The calculation period of both cases was from 0:00 JST on August 4 to 0:00 JST August 8. Numbers of domains differ between the two calculations. Both calculation areas are shown in Figure 4. Case A has three domains with one-way nesting and horizontal resolutions of 4500 m, 1500 m and 500 m. Case B has only one domain: the whole calculation area is smaller than Case

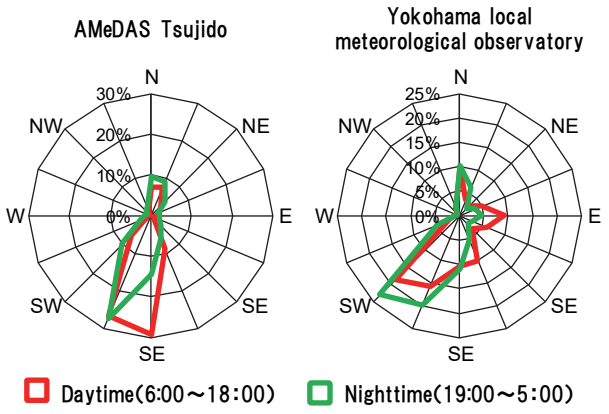

Fig. 2 Wind roses of AMeDAS Tsujido and YLMO. These figures were made using data of summer, 2011–2015.

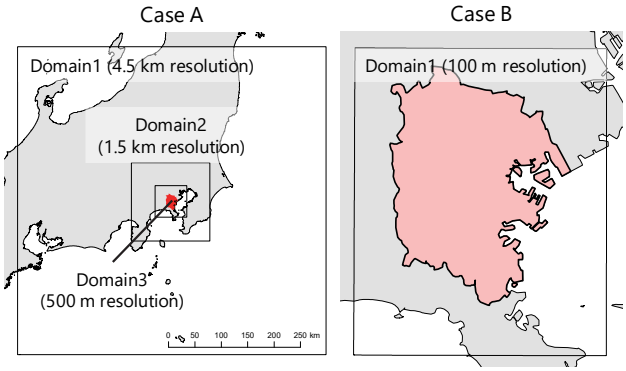

Fig. 4 Calculation areas of Case A and Case B. Numbers of domains and whole covered areas are different among two calculations.

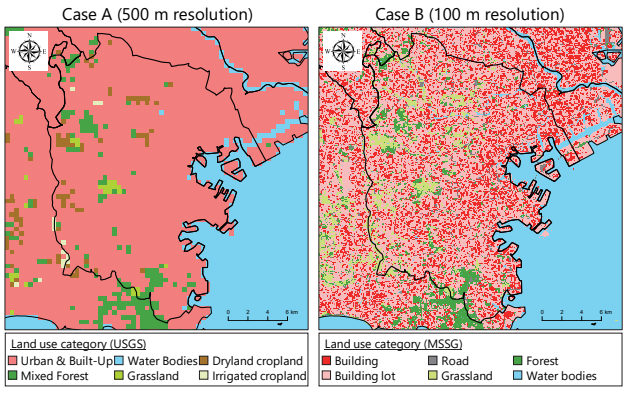

Fig. 5 Land use map of Case A and Case B. Land uses in both cases are classified into six categories.

A. The input dataset is mainly land use, elevation, and the green fraction (only in the WRF model). Figure 5 presents the land use maps of the two cases. Land use categories are classified based on USGS classification in Case A, and are classified into six categories in Case B, as shown in Figure 5. As an original land use dataset, National Land Numerical Information is used in both cases. Furthermore, results of Basic Survey of City

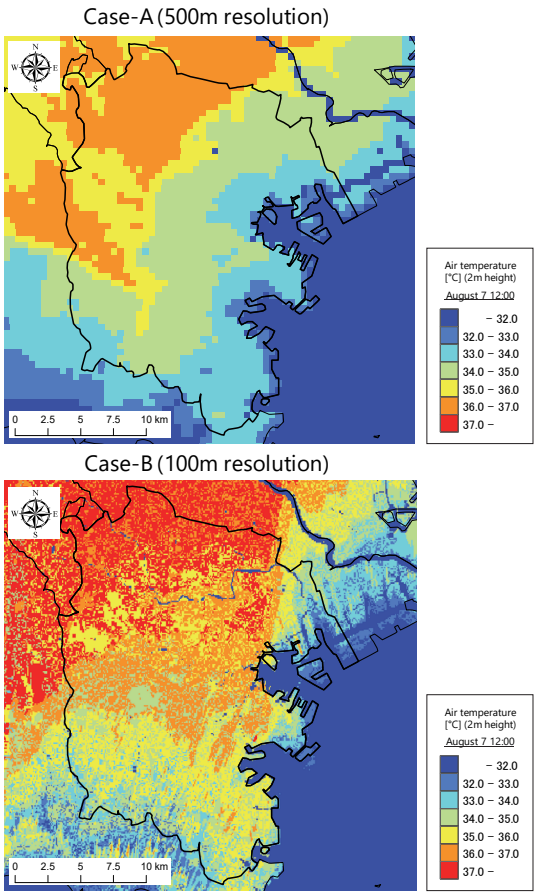

Fig. 6 Horizontal air temperature distribution at 12:00 JST, August 7 (2 m above ground). The distribution tendency is similar to observation results. However, the shapes of high air temperatures differ between the two cases. This difference seems to result from differences of the wind direction of sea breezes from Sagami Bay.

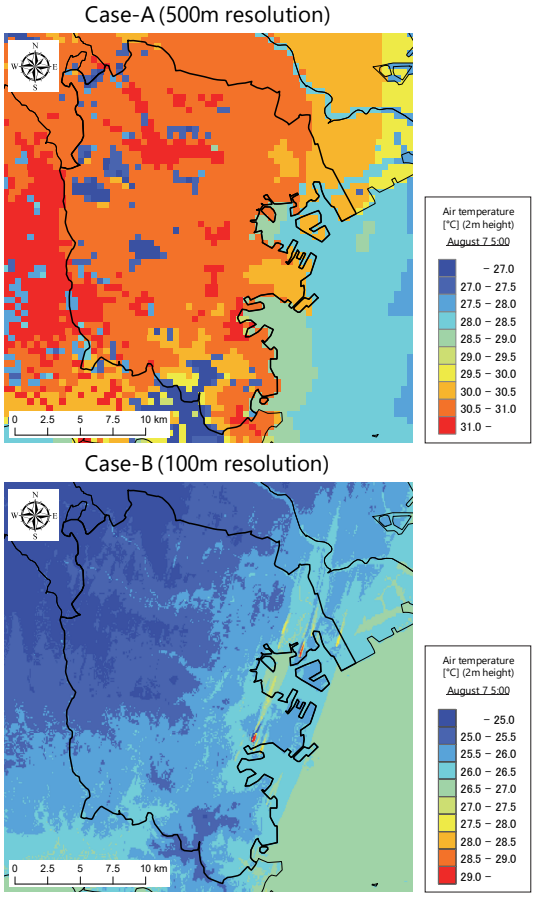

Fig. 7 Horizontal air temperature distribution at 05:00 JST, August 7 (2 m above ground). Absolute values are different between Case A and Case B. In Case B, air temperature is lower in inland area and distribution patterns are defined along topographical charateristics.

Planning in Yokohama are used to identify building meshes in Case B. In addition, a single-layer urban canopy model [11] is introduced for Case A and Case B. Therefore, building effects such as anthropogenic heat and reduction of wind speed in the urban area are considered. In Case A, anthropogenic heat is emitted equally from urban meshes. However, anthropogenic heat is defined for every urban meshes including from housing, roads, and factories in Yokohama in Case B. Therefore, we should take care when analyzing results outside of Yokohama in Case B.

3. Results and discussion

3.1 Air temperature distribution

Here, horizontal air temperature distributions from two calculation results are presented. We compared their distributions. Figure 6 shows horizontal air temperature distributions at 12:00 JST on August 7 (2 m above the ground). In both cases, the air temperature is lower in the coastal area, becoming gradually higher toward inland areas. Additionally, air temperatures are highest around the northwestern part of Yokohama, reaching over 36°C. These distribution patterns are mainly the same as those of observation results presented in the previous section.

From comparison among two cases, air temperature was mostly higher in Case B than in Case A. Furthermore, the shapes of high air temperature areas differed among these cases. In Case A, air temperatures gradually became higher not only from Sagami and but also from Tokyo Bay. However, in Case B, part of the high air temperature area extends near the coastline of Tokyo Bay. The cooler area along Tokyo bay is smaller than that in Case A. This difference seems to derive from differences of sea breeze effects from Tokyo Bay between the two calculations. Actually, the wind direction from Tokyo Bay in Case B is not east, but almost south, which seems to result from the single domain setting in Case B. This case cannot reflect the local wind environment adequately. Consequently, increasing the number of domains and improving calculations using MSSG model is a subject for future work.

Figure 7 shows horizontal air temperature distributions at 5:00

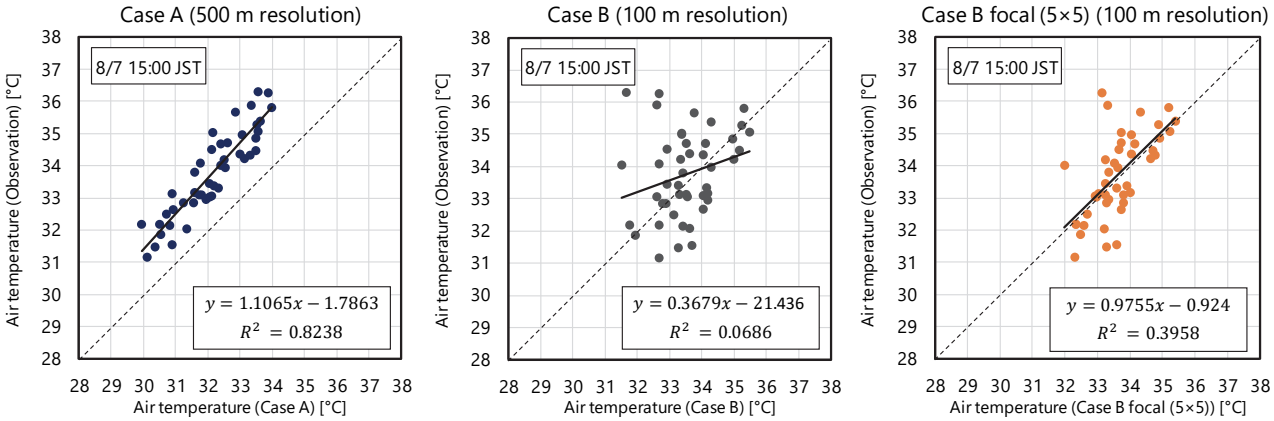

Fig. 9 Scatter plots of air temperatures between calculation and observation results at 15:00 JST on August 7. Plot of Case B focal (5×5) is distributed along the dotted line without some observation points.

JST on August 7 (2 m above the ground). Air temperature differences in urbanised areas are about 1.5°C-2.0°C and smaller than that of daytime in both cases. However, absolute values are different between Case A and Case B. Air temparature of Case A is about 5°C higher than that of Case B. Case A overestimate about 2°C and Case B underestimate about 2°C compared to observation result (figure 3). Calculation accuracy of absolute values are need to be improved in the next challenge. With regard to distribution tendency, air temperatures in coastal area are lower in Case A; higher in Cases B. In addition, air temperatures in inland area are lower and air temperature differences are shown along valley lines. This result seems that high resolution calculation can consider topographical effect more clearly. As a result, effect of sky radiation cooling on air temperature distribution in inland area is more remarkable in this case.

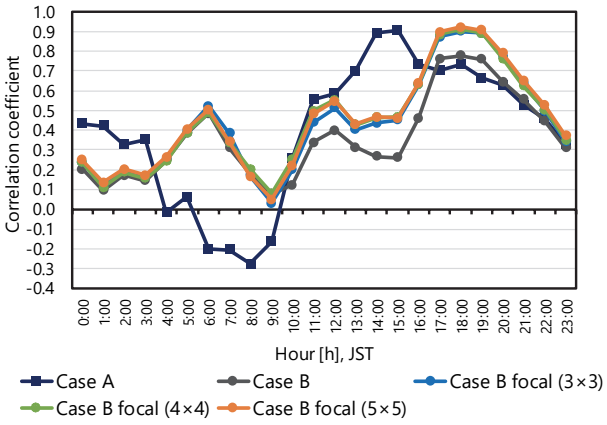

Fig. 8 Hourly correlation coefficients of cases of August 7. Correlation coefficients are higher during daytime and lower during nighttime. During nighttime, correlation coefficients of high-resolution cases are higher than those of Case A.

3.2 Comparison with observation results

Here, calculation results are compared with observation results. In the next section, we classify urban meshes using cluster analysis. Cluster analysis classify all samples into some groups based on relative magnitude correlation. So, important point of calculation accuracy is to what extent these calculations can express relative magnitude correlation among each observation points. Therefore, we mainly calculated correlation coefficients of respective cases with observation results to analyze such relative magnitude correlation in each calculation. For this comparison, only 45 observation points located in Yokohama and calculation results of 45 meshes located at respective observation points were used.

Figure 7 presents hourly correlation coefficients for August 7. In this figure, three additional results were obtained using smoothed values of Case B are also shown. Here, Case B focal (3×3) represents the averaged values by surrounding nine meshes using results of Case B are used. In addition, Case B focal (4×4) and Case B focal (5×5) respectively use values averaged by the surrounding 16 and 25 meshes. As shown figure 7, correlation coefficients are higher during daytime than nighttime in all cases. In addition, correlation coefficients are lower in Case B than in Case A during daytime. Air temperatures are sparsely distributed because of detailed temperature reduction effects by sea breezes and land use effects in Case B. In three smoothed cases, correlation coefficients are generally higher than in Case B during daytime. However, an increase of correlation coefficients is independent of the number of meshes used for smoothing. Correlation coefficients are smaller during nighttime according in figure 7. Especially, correlation coefficients are negative in Case A from midnight to morning. This is because that air temperature differences in nighttime are smaller in calculation results as shown figure 7. Besides, beginning of blowing sea breeze in the morning is earlier in calculation result of Case A. So, air temperature distribution tendency become converse between observation and calculation

results in Case A in the morning. However, correlation coefficients are higher in Case B than in Case A at that time. During nighttime, effects of land use and topography on air temperatures are generally more remarkable than during daytime. Therefore, Case B seems to reflect nighttime air temperatures more correctly than Case A.

This result shows that using high-resolution calculation using MSSG result model is apparently improve calculation accuracy of relative magnitude correlation and effective to calculate the urban climatic environment during nighttime and to produce climatic zoning maps that include nighttime effects.

For analyzing decrease of correlation coefficients in case A during the daytime, we made scatter plot among calculations and observation results. Figure 8 depicts a scatter plot of air temperatures at 15:00 JST on August 7 made using calculations and observation results at 45 points. From this Figure, the coefficient of determination was found to be higher in Case A than in Case B and Case B focal (5×5) at 15:00 JST on August 7. The plots are sparsely distributed in Case B compared with Case A. However, most of plots are concentrated along the dotted line in Case B focal (5×5). Furthermore, some plots is located far from the dotted line in Case B focal (5×5). These observation points are located downwind factories in a coastal area of Tokyo Bay and seems to be affected from anthropogenic heat. As mentioned above, wind directions of the sea breeze from Tokyo Bay in Case B is incorrect and this seems to generate underestimation in some observation points in high-resolution calculation. This result shows that the air temperature calculated using the high-resolution case has some dispersion, but relative magnitude correlation is calculable correctly during daytime using average values with surrounding meshes.

From these results, high-resolution calculation seems to be possible and effective for making more detailed climatic zoning maps. In the next chapter, we produce climatic zoning maps using two calculation results are different on calculation accuracy of relative magnitude correlation.

3.3 Climatic Zoning in Yokohama

Earlier sections describe that the calculate accuracy of relative magnitude correlation of two calculations are analyzed through comparison with observation results. Furthermore, utilization possibilities of high-resolution calculations for making climatic zoning maps were found.

Therefore, hierarchical cluster analysis is performed to classify urban area in terms of urban climate using two calculation results. Cluster analysis is the statistical method classifying many samples into some groups by resemblance of each samaple. In this analysis, resemblance between each samaple are defined as distance. At first, most similar pair of samples are summarized and first cluster is generated. Resemblance between first cluster and other cluster or sample is calculated again and number of clusters is reduced in order. Finally, tree diagram showing clusters classified based on resemblance of all samples are provided. In this study, squared Euclidean distance is used as measuring scale of resemblance between each sample. As constructing method of cluster, Ward method constructing clusters based on dispersion in or among groups is used. Samples are urban meshes (i.e. Urban & Built-up in Case A and Building, building lot and Road in Case B) located in Yokohama. Actually, 1,657 meshes are used for Case A; 46,615 meshes are used for Case B focal (3×3). For these analyses, we used data of Case B focal (3×3) as the 100 m resolution case because of higher correlation coefficients than those in Case B in previous section. Cluster analysis used variables of 24 hourly air temperatures of August 7, 2015. We considered spatial distributions of hourly air temperature change characteristics are classified clearly by this setting. Number of cluster can be defined freely from analysis result in hierarchical cluster analysis. Here, we defined five clusters in this study reffering to YOKOHAMA CLIMAATLAS 2010(12).

Figure 9 shows a horizontal distribution of each zone. Figure 10 presents the hourly average air temperature of each zone. From Figure 9, the distribution of each zone is classified mainly based on the distance from coastal line of Sagami and Tokyo Bay in both cases. The urban climate in Yokohama is affected strongly by sea breezes during daytime. Additionally, distribution patterns of the respective zones are similar between Case A and Case B. Nevertheless, the shapes of respective zones are partly defined according to topography and natural areas such as valleys and downward slopes of green areas in Case B focal (3×3). Therefore, more detailed climatic zoning will be possible using high resolution for wide-area numerical calculations with a MSSG model.

Figure 10 shows that the maximum air temperature is highest in Zone 5 an inland area in both cases. The maximum air temperature is the lowest in Zone 3, a coastal area of Tokyo Bay. As shown in Figure 10, the times of maximum air temperature differ among zones in Case A. This time is defined as that when a sea breeze from Sagami Bay arrives at each zone. Therefore, such times of Zone 1 and Zone 2 locating near Sagami Bay are earlier than those other zones. In addition, air temperatures in the morning are lower than those in other areas in Zone 3 and Zone 4 located in coastal areas of Tokyo Bay because sea breezes from Tokyo Bay blow in the morning. However, temporal differences of maximum air temperature times among zones do not exist in Case B focal (3×3). Apparently, the temporal change of sea breezes from Sagami Bay and Tokyo Bay are not reflected in this case compared to Case A. Most of the southern part of Yokohama and part of the coastal area of Sagami Bay are included in same zone (Zone 1) in Case B focal (3×3).

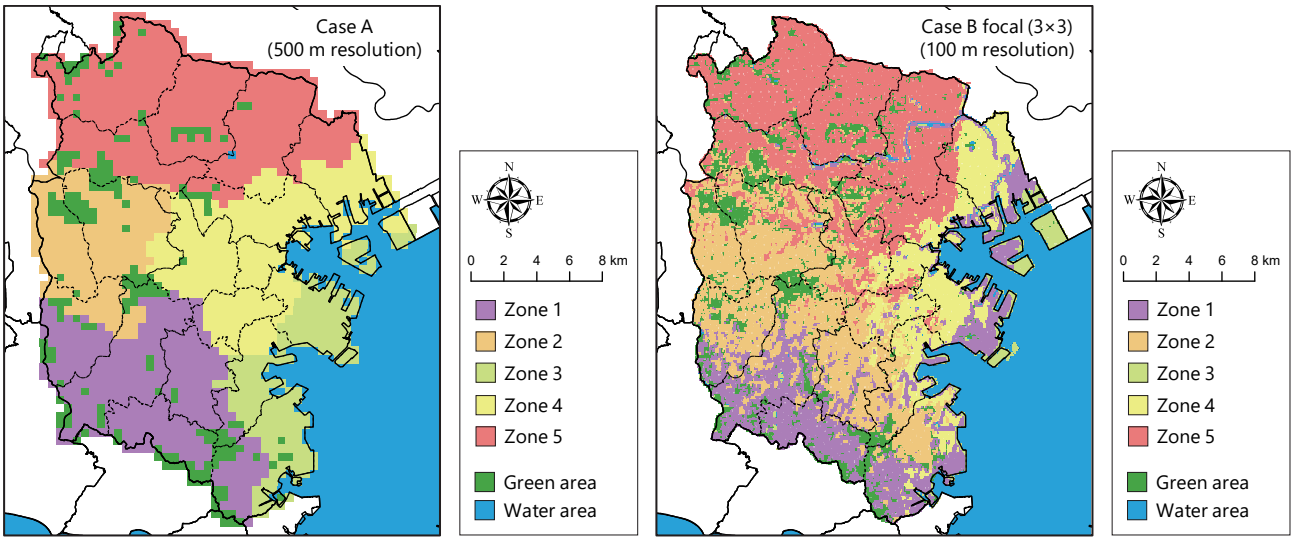

Fig. 10 Horizontal distribution of each zone: (left) Case A (500 m resolution) (right) and Case B-focal (3×3) (100 m resolution). Distributions of the five zones are similar, but each zone of Case B focal (3×3) is partly shaped along the topography and the green area.

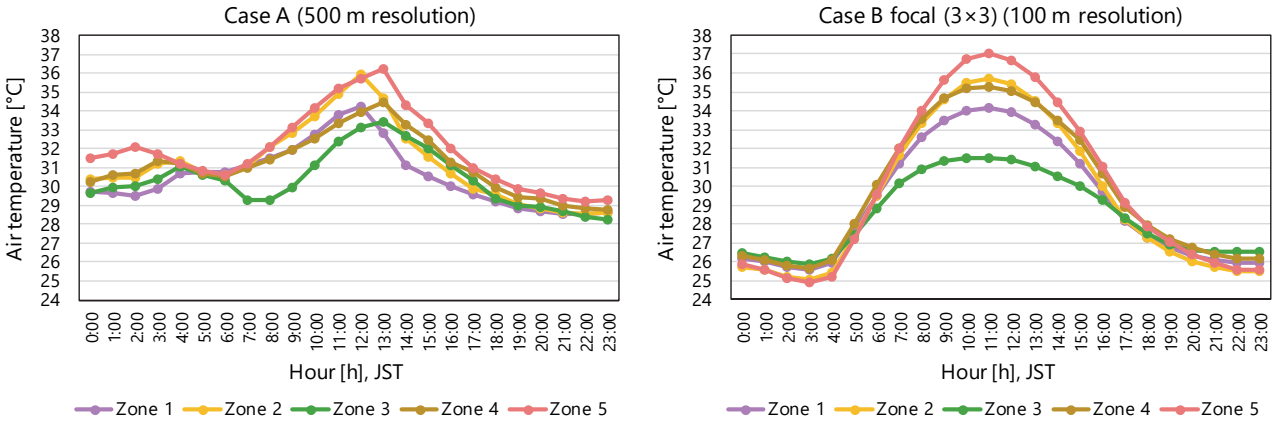

Fig. 11 Hourly average air temperature of each zone: (left) Case A (500 m resolution) and (right) Case B (100 m resolution). Time of maximum air temperature differs in Case A, but it is almost identical in Case B-focal (3×3).

4. **Summary**

For this study, calculations of two kinds were executed using a WRF model with 500 m resolution and an MSSG model with 100 m resolution to show that climatic zoning maps made from high-resolution calculation are effective because of including detailed information. Furthermore, each calculation result was compared with observation results to analyze calculation accuracy of relative magnitude correlation. In addition, climatic zoning maps were produced from calculation results obtained using cluster analysis. The major findings are presented below.

1) High-resolution case can reflect detailed effects of topography and land use and improve calculation accuracy of relative magnitude correlation during the nighttime.

2) High-resolution case has some dispersion, but relative magnitude correlation is calculable correctly during daytime using average values with surrounding meshes.

3) Distribution patterns of respective classified zones are mostly the same among two climatic zoning maps. However, some zones were partly distributed along topography and natural areas in the high-resolution case. Therefore, using a high-resolution case is apparently effective to produce more detailed climatic zoning maps.

Future works will address the following objectives.

1) Increasing the number of domains and expanding the calculation areas of high resolution calculations using the MSSG model are necessary to reflect local wind environments such as sea breezes from Tokyo Bay in the morning.

2) Expansion of the calculation period and use of the average of some sunny days are necessary for each analysis.

3) Consideration of suitable countermeasures is necessary for each zone to mitigate urban warning effects.

Acknowledgements

This study was supported by JSPS KAKENHI grant number JP16J03661. This study was also supported by a grant of the Asahi Glass Foundation. For numerical calculation, this study

used Earth Simulator, with the support of JAMSTEC.

References

(1) T. Tanaka, K. Yamazaki and M. Moriyama, Urban Environmental Climate Maps for Supporting Environmental and Urban Planning Works in Local Government: Case Study in City of Sakai, Osaka, Summaries of Technical Papers of Annual Meeting Architectural Institute of Japan, D-1 (2008), pp.207-210. (in Japanese)

(2) S. Iizuka, Y. Kondo and Y. Xuan, Introduction of Disaster-Mitigation/Prevention Type Urban Structure Models and Their Impacts on Thermal Environment: Numerical Study on Thermal Environment in the Nagoya Metropolitan Area by Using WRF (Part 5), AIJ Journal of Environmental Engineering, 79-694 (2014), pp.883-889. (in Japanese)

(3) G. Papangelis, M. Tombrou, A. Dandou and T. Kontos, An urban "green planning" approach utilizing the Weather Research and Forecasting (WRF) modeling system: A case study of Athens, Greece, Landscape and Urban Planning, 105-(1-2) (2012), pp.174-183.

(4) N. Kitao, M. Moriyama, H. Takebayashi and T. Tanaka, A study on making method of climate atlas in Osaka region, AIJ Journal of Technology and Design, 18-38 (2012), pp.255-258. (in Japanese)

(5) H. Oba, T. Yoshida, A. Mochida, H. Yoshino and H. Watanabe, Zoning of the urban climate in Sendai for selecting the appropriate countermeasures against urban heat island effects, Proceedings of the 19th national symposium on wind engineering (2007), pp.55-60. (in Japanese)

(6) K. Matsuo, T. Tanaka, Analysis on the effect of sea breeze on summer diurnal temperature distribution pattern in Hiroshima plain -Mapping the sea breeze effects for mitigating urban warming-, AIJ Journal of Environmental Engineering, 81-721 (2016), pp.283-293. (in Japanese)

(7) Y. Sasaki, K. Matsuo, M. Yokoyama, M. Sasaki, T. Tanaka, S. Sadohara, Factors affecting summer temperature distributions in a coastal city and surrounding area -Long-term, multi-point measurement analysis of Kanagawa Prefecture-, Journal of the City Planning Institute of Japan, 51-3 (2016), pp.596-602. (in Japanese)

(8) Y. Matsushima, T. Ogura, R. Yamashita, J. Naito and K. Seki, Results of air temperature in the summer of 2013-2015 in Yokohama -Mitigation effect on rise in air temperature by greenery area, Annual Report of Yokohama Environmental Science Research Institute, 41 (2017), pp.25-32.

(9) W.C. Skamarock, J.B. Klemp, J. Dudhia, D.O. Gill, D.M. Barker, M.G. Duda, X.-Y. Huang, W. Wang and J.G. Powers, A description of Advanced Research WRF Version3, NCAR Technical Note, (2008).

(10) K. Takahashi, R. Onishi, Y. Baba, S. Kida, K.Matsuda, K. Goto and H. Fuchigami, Challenge toward the prediction of typhoon behaviour and down pour, Journal of Physics: Conference Series, 454-1 (2013).

(11) H. Kusaka and F. Kimura, Coupling a single-layer urban canopy model with a simple atmospheric model, Impact on urban heat island simulation for an idealized case, Journal of the Meteorological Society of Japan, 82-1 (2004), pp.67-80.

(12) T. Tanaka, S. Sadohara and S. Inachi, Urban Environmental Climate Maps for Planning and Design: Trials in Yokohama, Proceedings of the 8th International Symposium on Architectural Interchanges in Asia, Kitakyushu (2010), P-09 (CD-ROM).

(Received Apr. 30, 2017, Accepted Jul. 7, 2017)